Journal of Hazardous Materials, 30 (1992) 297–316
Elsevier Science Publishers B.V., Amsterdam

The effect of sodium sulfate on solidification/stabilization of a synthetic electroplating sludge in cementitious binders

Amitava Roy[a], Harvill C. Eaton[a], Frank K. Cartledge[b] and Marty E. Tittlebaum[a]

Colleges of [a]Engineering and [b]Basic Sciences, Louisiana State University, Baton Rouge, LA 70803 (USA)

(Received July 15, 1991; accepted in revised form October 25, 1991)

Abstract

The effect of sodium sulfate on the solidification/stabilization of a large quantity of a synthetic electroplating sludge in cementitious binders was studied. The sludge was dewatered to 25% solids and contained 86.2 mg/g Ni, 84.1 mg/g Cr, 18.8 mg/g Cd, and 0.137 mg/g Hg. Three stabilizing mixtures were investigated: Type I portland cement (also called ordinary portland cement, OPC) (OPC to sludge ratio = 0.3 to 1), OPC and Class F fly ash (OPC to fly ash to sludge ratio = 0.2 to 0.5 to 1), Class C fly ash and lime (lime to fly ash to sludge = 0.3 to 0.5 to 1). Sodium sulfate was added in amounts equal to 0 (control), 2, 5 and 8% by weight of solidified binder. A set of binder samples without the sludge, but containing 8% sodium sulfate, was also prepared for comparison. The microstructure, microchemistry and phases were studied by scanning electron microscopy, energy dispersive X-ray spectroscopy, and X-ray diffractometry. The chemical species in the sludge were not significantly affected by sodium sulfate, but the binders reacted with the interfering compound. The amount of ettringite in all samples was proportional to the sodium sulfate content. The fraction of crystalline compounds in the binders increased with sodium sulfate concentration, and new compounds containing Na, Ca, S, Al, and Si were formed. Apart from prisms of ettringite, different crystalline forms were found in each binder. For the same level of sodium sulfate (8%), the crystalline forms and microstructure in a sample depended on the presence or absence of sludge.

1. Introduction

Solidification/stabilization (S/S) by the formation of a cementitious solid is a common, economical method for treatment, prior to disposal, of hazardous chemical wastes [1]. The cementitious binder can be Type I portland cement (which we call ordinary portland cement–OPC) or OPC with admixtures such as Class C or F fly ash. Additives such as sodium silicate are often added to

Correspondence to: Dr. H.C. Eaton, College of Engineering, Louisiana State University, Baton Rouge, LA 70803 (USA).

improve performance at particular set times, but may also affect the leachability of the waste. The exact mechanism of entrapment and the long term behavior in different chemical environments, however, are poorly understood.

Most studies have considered the mechanical properties or leaching behavior of the solidified waste. In contrast, our work aims at understanding the chemical or physical mechanisms of S/S. In early works we focused primarily on simple, model waste systems [2,3], but recently we have considered more complex systems. For example, physical encapsulation was determined to be the primary mechanism of stabilization in a mixture of synthetic electroplating waste (EPA classification F006) and portland cement/Class F fly ash [4]. The present study considers the effect of sodium sulfate, a widely used industrial chemical, on S/S of the same synthetic electroplating waste in three cementitious binders. Apart from heavy metals, the waste stream from an electroplating operating contains compounds used for cleaning and washing, which may adversely affect the performance of a binder during S/S. Therefore, the results of this investigation should provide information useful to designers of more effective S/S schemes.

2. Experimental procedure

A synthetic heavy metal sludge was prepared from chromium, nickel, cadmium and mercury nitrates. The heavy metals were precipitated as insoluble hydroxides by adding lime to water containing the nitrates. The sludge was dewatered to 25% solids, poured into three 567 L (150 gallon) drums, and solidified by the addition of Type I portland cement, portland cement and Class F fly ash (CFA), and Class C fly ash and lime (LFA) (see Table 1; details are found in Cullinane et al. [5]). After the sludge was mixed with each binder, the mixture was divided into four equal parts and sodium sulfate was added at 0 (control), 2, 5 and 8% by weight of binder/sludge. Samples of binders with 8% interfering compound, but without sludge, were also prepared. After curing under ambient conditions for six months to one year, they were studied by scanning electron microscopy (SEM), energy dispersive X-ray spectroscopy (EDX), and X-ray diffractometry (XRD) using methods described previously [2,3]. Scanning electron microscopy and semiquantitative energy dispersive X-ray analysis were performed with an ISI-60A scanning electron microscope equipped with an EDAX 9100 energy dispersive spectrometer. The SEM samples were coated with gold, and the EDX samples were coated with carbon.

X-ray diffractometry was performed with powdered samples, obtained by grinding with porcelain and agate mortars. Very few samples could be sieved because of their high moisture content. The XRD patterns were obtained with a Scintag Pad V automated diffractometer using Cu K_α radiation. The oper-

TABLE 1

Solidification/stabilization mixtures[a]

Binder	Sludge	Binder/sludge ratio	Sodium sulfate weight percentage
OPC (Type I portland cement)	Ni–86.2 mg/g, Cr–84.1 mg/g, Cd–18.8 mg/g, Hg–0.137 mg/g Sludge was dewatered to 25% solids	0.3/1 (OPC/sludge)	0, 2, 5 and 8
CFA (Type I portland cement and Class F fly ash)		0.2/0.5/1 (OPC/fly ash/sludge)	0, 2, 5 and 8%
LFA (lime and Class C fly ash)		0.3/0.5/1 (lime/fly ash/sludge)	0, 2, 5 and 8%

[a]See [5] for details of sample preparation.

TABLE 2

Symbols used for phases in XRD patterns

Symbol[a]	Phase[b]
A	Alumina (Al_2O_3)
Cc	Calcium carbonate ($CaCO_3$)
CAH	Calcium aluminate hydrate ($xCaO \cdot zAl_2O_3 \cdot yH_2O$)
CH	Calcium hydroxide ($Ca(OH)_2$)
C_2S	Dicalcium silicate ($2CaO \cdot SiO_2$)
C_3S	Tricalcium silicate ($3CaO \cdot SiO_2$)
Et	Ettringite ($3CaO \cdot Al_2O_3 \cdot 3CaSO_4 \cdot 32H_2O$)
Gyp	Gypsum ($CaSO_4 \cdot 2H_2O$)
Mag	Magnetite (Fe_3O_4)
Ml	Melilite ($Ca_2Al_2SiO_7$–$Ca_2MgSi_2O_7$) (solid solution between two end members)
MS	Monosulfate ($3CaO \cdot Al_2O_3 \cdot CaSO_4 \cdot 13H_2O$)
Mu	Mullite ($3Al_2O_3 \cdot 2SiO_2$–$Al_2O_3 \cdot SiO_2$)
Pe	Periclase (MgO)
Qu	Quartz (SiO_2)
Sp	Spinel ($(Mg, Cr, Fe)AlO_4$)

[a]Cement chemist's notation: C = CaO; A = Al_2O_3; S = SiO_2; and H = H_2O.
[b]x, y and z are variable.

ating conditions for the X-ray examinations were: 45 keV accelerating voltage, 35 mA current, 3 to 70° 2Θ-scanning range, 0.02° step-width, and a minimum of 3 seconds counting time or 3000 counts. The widths of slits positioned before the sample were 2° and 4°, and those after the sample were 0.5° and 0.3°. The sample holder was spun on its vertical axis to minimize the effect of the het-

erogeneous composition, grain size, orientation and texture. Synthetic corundum (5 μm) and quartz from fly ash were used as internal standards in sludge and ash-containing binders, respectively. Abbreviations used for phases identified in XRD patterns are given in Table 2.

3. Results

3.1 Type I portland cement

In the SEM, OPC/sludge with 0% sodium sulfate had a granular, sometimes layered, appearance. When 2% sodium sulfate was added to OPC/sludge, cubic crystals with cubic and octahedral faces formed. An example is shown in Fig. 1. As shown in Fig. 2, the crystals, a few μm in diameter, became more abundant in OPC/sludge with 5 and 8% sodium sulfate, but the faces were not as distinct and well-formed. With increasing amounts of sodium sulfate, there was also a proportionate increase in the formation of long prismatic ettringite crystals as shown in Fig. 3. Thin to massive plates with hexagonal symmetry were common in OPC/sludge with 2% sodium sulfate, as well as oblately-shaped calcium silicate grains, 50–60 μm long, surrounded by very fine grained reaction products.

With 8% sodium sulfate content, the microstructure was different when the sludge was absent. As seen in Fig. 4, which shows a sample containing no sludge, massive hexagonal plates developed and the prismatic ettringite needles were considerably thinner than in samples which contained sludge. Also, the cubic crystalline form failed to develop in OPC with 8% sodium sulfate.

Analyses of the cubic crystals from OPC/sludge with 5 and 8% sodium sulfate are shown in Figs. 5(a)–5(c). The crystals showed widely varying compositions, but the same elements, including waste elements, were always present. Figure 5(d) shows an analysis of ettringite. The analysis reveals that along with Ca and S, a significant amount of Si replaced Al in the crystal. An analysis of the massively layered region from OPC with 8% sodium sulfate seen in Fig. 4 is shown in Fig. 5(e). Minor amounts of Si, Na, Al and S were present. Analyses of the matrix of OPC/sludge samples showed heavy metals at low concentrations.

Figure 6 shows XRD patterns of (a) the sludge, (b) hydrated OPC, (c–f) OPC/sludge with increasing amounts of sodium sulfate, and (g) OPC with 8% sodium sulfate. The hydration products calcium hydroxide and ettringite were observed in all samples and the amounts of ettringite, C_3S, and C_2S increased with sodium sulfate concentration. Gypsum was only found in OPC/sludge containing 8% sodium sulfate. Varying amounts of calcite were present in all samples. Most peaks that were present in the sludge, particularly at low 2Θ values, were found in samples containing both waste and sodium sulfate, though their intensities varied widely (compare Fig. 6(a) with Figs. 6(b) and 6(c)–

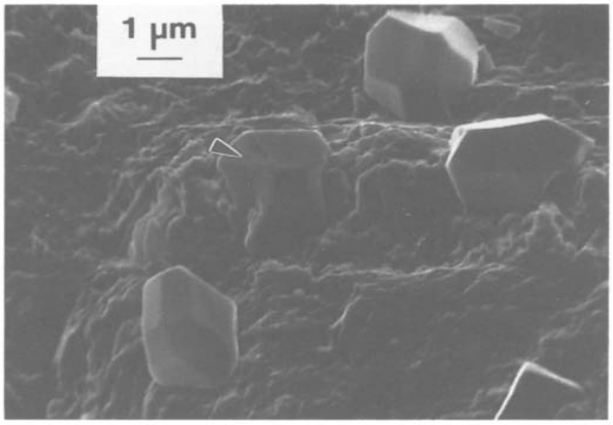

Fig. 1. SEM picture of OPC/sludge treated with 2% (w/w) Na_2SO_4.

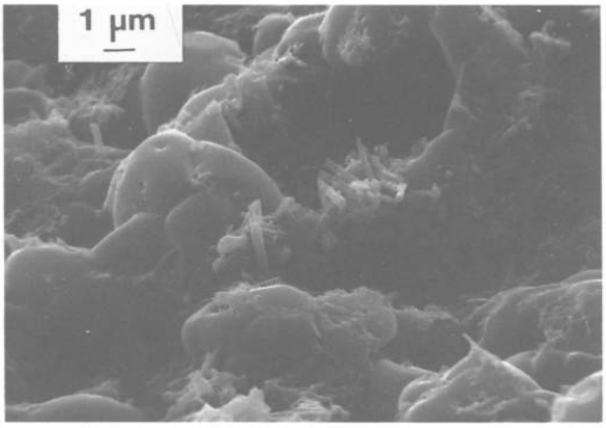

Fig. 2. SEM picture of OPC/sludge treated with 5–8% (w/w) Na_2SO_4.

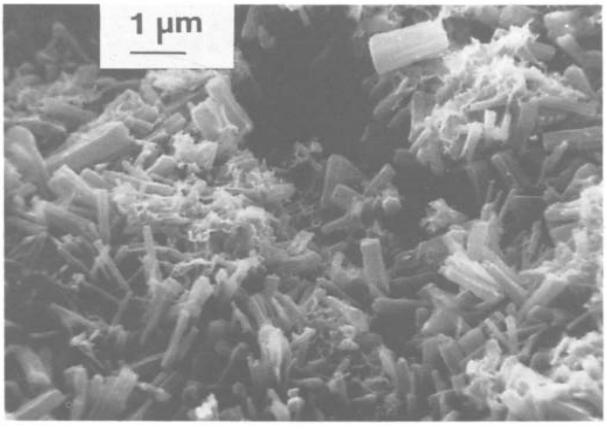

Fig. 3. SEM picture of OPC/sludge treated with over 8% (w/w) Na_2SO_4.

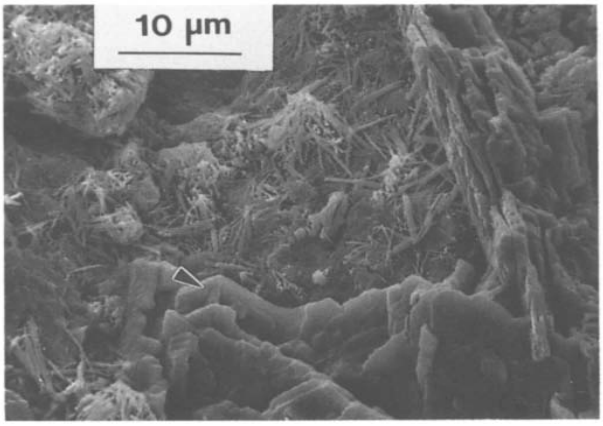

Fig. 4. SEM picture of OPC (without sludge) treated with 8% (w/w) Na_2SO_4. Note the different magnification and the increase in the number of long crystals.

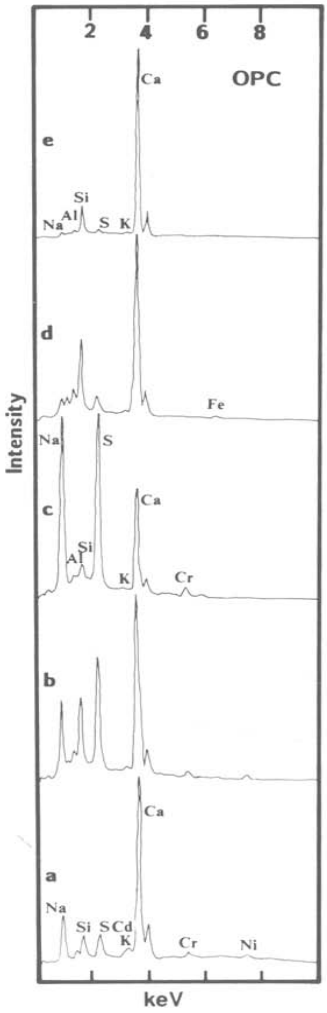

Fig. 5. Energy dispersive X-ray analysis of the cubic crystals from OPC/sludge with 5 and 8% (w/w) Na_2SO_4 addition (a–c), and ettringite (d). In (e) an analysis of the massive layered region formed in Fig. 4 is shown.

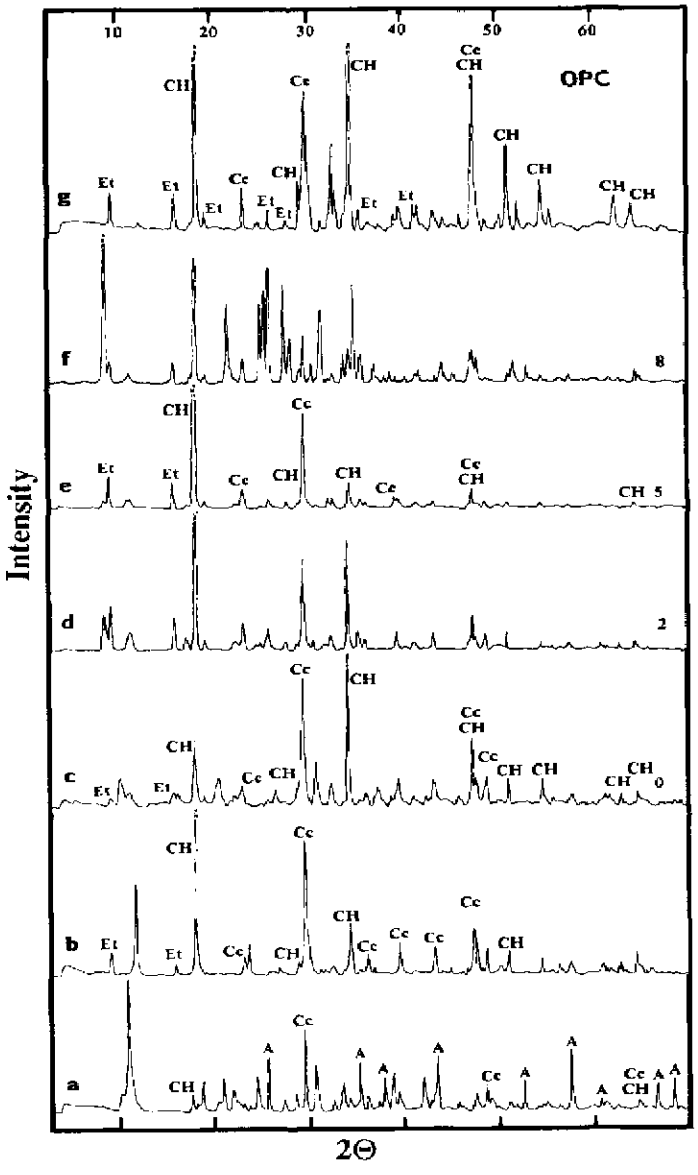

Fig. 6. XRD patterns of the sludge (a), hydrated OPC (b), OPC/sludge with increasing amounts of Na_2SO_4 (c–f) and with 8% (w/w) Na_2SO_4 (g).

6(f)). The most intense sludge peak ($\approx$0.800 nm) remained prominent in all OPC/sludge samples, independent of sodium sulfate concentration (Fig. 7). The shoulder ($\approx$0.860 nm) on the low-angle side of the main sludge peak was very intense in the OPC/sludge sample containing 0% sodium sulfate, but it disappeared as the amount of the interfering compound in the sample increased.

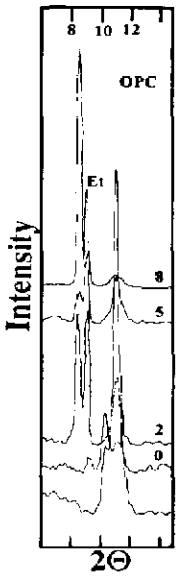

Fig. 7. The intensity of the sludge peak at 0.8 nm is independent of the amount of Na_2SO_4.

3.2 Type I portland cement/Class F fly ash (CFA)

In the SEM, at magnifications greater than 1000×, the matrix of the CFA/sludge containing 0% sodium sulfate consisted of thin plates, a few tenths of a micrometer thick. Figure 8 shows that the addition of 2% sodium sulfate did not make a perceptible difference, but, as shown in Fig. 9, with 5% sodium sulfate the amount of ettringite increased.

CFA/sludge with 8% sodium sulfate was distinctly different. In addition to more hexagonal prismatic ettringite crystals, the matrix consisted of thick parallel plates with smoothly varying boundaries, as shown in Fig. 10. Fly ash spheres showed varying degrees of reaction, independent of the amount of interfering compound.

Figure 11 reveals that the microstructure of CFA with 8% sodium sulfate was unlike that with the sludge. In the absence of the sludge, the fraction of crystalline phases was small and the ettringite crystals were thinner. A similar observation was also made for OPC with 8% sodium sulfate.

Apart from prismatic forms of ettringite, the crystalline forms observed in CFA/sludge with different amounts of ettringite were different from those in OPC/sludge with similar concentrations of sodium sulfate.

An analysis of an ettringite crystal from CFA/sludge with 5% sodium sulfate is shown in Fig. 12(a). Ca, S, Si, Al, Na and some waste elements were present. An analysis (Fig. 12(b)) of a similar crystalline form in CFA/sludge with 8% sodium sulfate shows that the same elements were present, but S, Si and Na had higher concentrations. The plate-like matrix of CFA/sludge with 5% so-

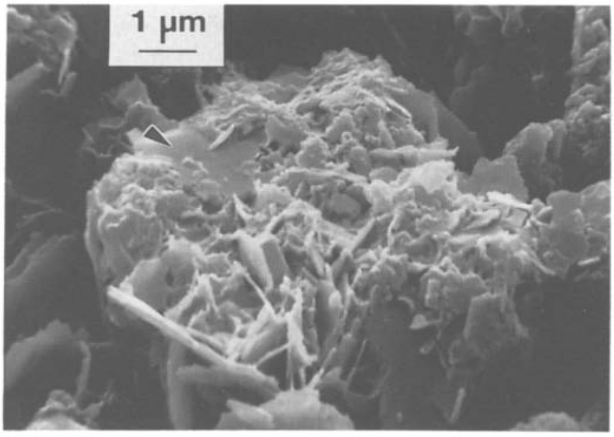

Fig. 8. SEM picture of Type I portland cement/Class F fly ash stabilized sludge treated with 2% (w/w) Na_2SO_4.

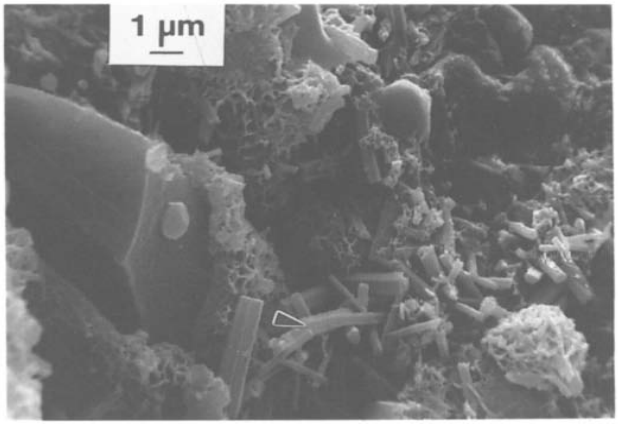

Fig. 9. SEM picture of Type I portland cement/CFA stabilized sludge treated with 5% (w/w) Na_2SO_4. Note the increase in ettringite amount as compared to Fig. 8.

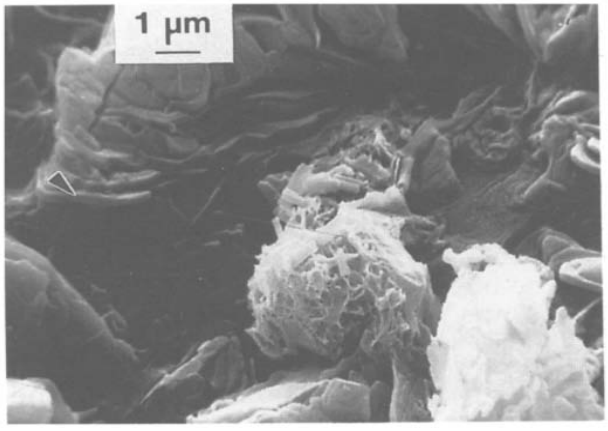

Fig. 10. As Fig. 9 but with 8% (w/w) Na_2SO_4 added. Note the thick parallel plates and the smooth boundaries.

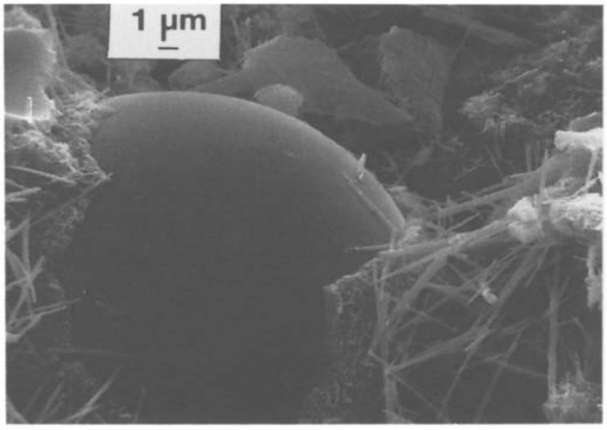

Fig. 11. Microstructure of CFA, without sludge, treated with 8% (w/w) Na_2SO_4.

dium sulfate contained all the elements expected to be in the binder, the waste, and the interfering compound, as shown in Fig. 12(c). Figure 12(d) shows the chemical composition of the platy matrix in CFA/sludge with 8% sodium sulfate (Fig. 10). Analyses of fly ash spheres from CFA/sludge with differing amounts of sodium sulfate indicated that Ca, Si and Al were the principal elements. The heavy elements were always present in minor quantities on the fly ash surfaces, as shown in Figs. (12(e) and 12(f), which are analyses of 0 and 8% samples, respectively.

XRD patterns of (a) sludge, (b) Class F fly ash, (c) CFA, (d–g) CFA/sludge with 0–8% sodium sulfate, and (h) CFA with 8% sodium sulfate, are shown in Fig. 13. The phases identified from the XRD patterns of CFA/sludge were from three groups:

1. Those from Class F fly ash
2. Those due to hydration of CFA
3. Those from sludge.

Mullite, quartz and occasionally iron oxides were present and due to the Class F fly ash (see Fig. 13(b)). Among the hydration products, ettringite was most pronounced in all samples with peak intensities increasing with increasing sodium sulfate concentration. Hydrogarnet (C_3AH_6) was found in CFA/sludge with 8% sodium sulfate. Monosulfate was observed in CA with 8% sodium sulfate. Unhydrated C_2S and C_3S were observed in all samples. Calcium hydroxide was absent as a hydration product in all CFA/sludge samples; it was present in CFA (Fig. 13c) and CFA with 8% sodium sulfate (Fig. 13h). A variable amount of calcite was present in all samples. A comparison of the XRD patterns of sludge, CFA and CFA/sludge with 0–8% sodium sulfate and CFA with 8% sodium sulfate shows that several peaks from the sludge, partic-

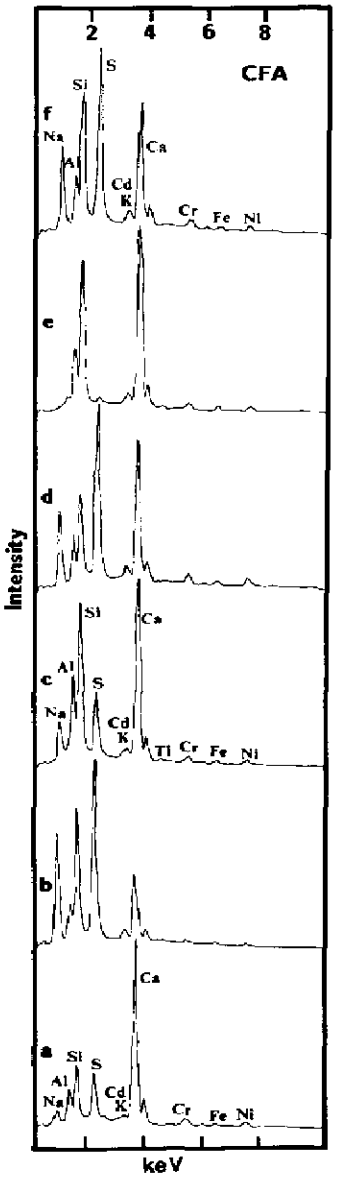

Fig. 12. Energy dispersive X-ray analysis pattern of an ettringite crystal of CFA/sludge treated with (a) 5% (w/w) Na_2SO_4, (b) 8% (w/w) Na_2SO_4, (c) and (d) are the respective analyses of the chemical composition of plate-like matrices, and (e) and (f) show the analyses of the fly ash spheres from CFA/sludge treated with 0 and 8% (w/w) Na_2SO_4, respectively.

ularly those at low 2Θ, could be found in CFA/sludge, but their intensities were variable. Similar to the OPC/sludge patterns, several unknown peaks remained.

3.3 Lime/Class C fly ash (LFA)

SEM showed that the bulk of LFA/sludge with 0% sodium sulfate consisted

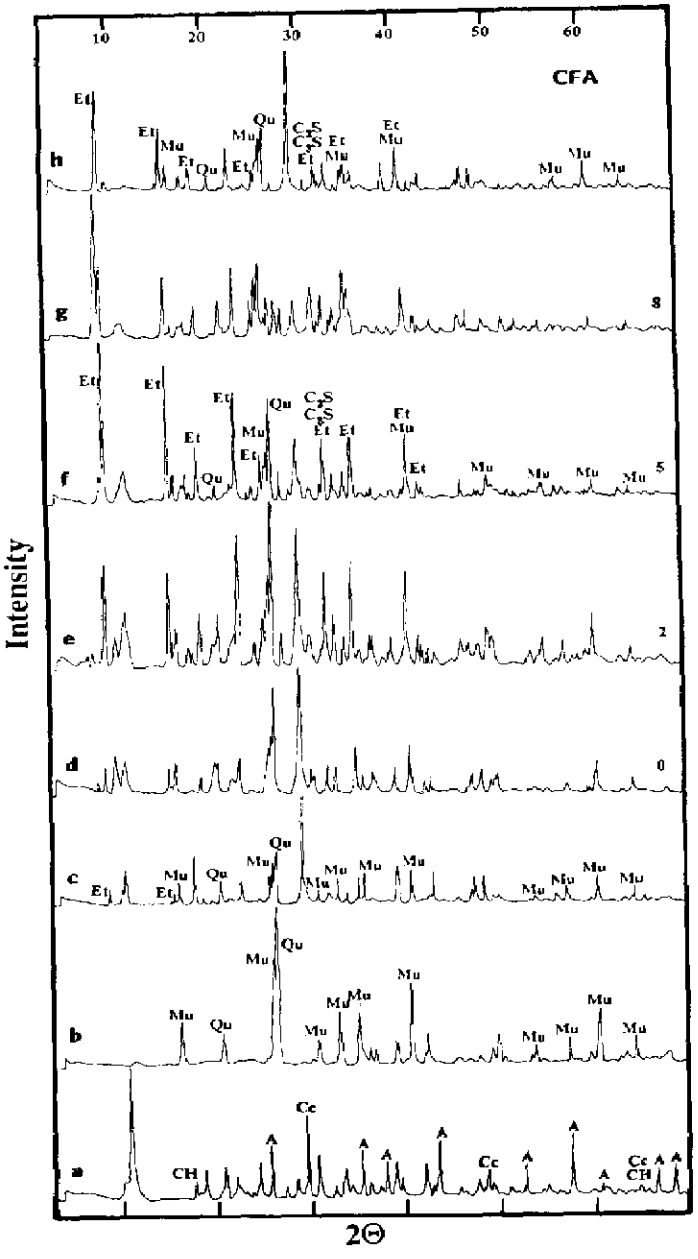

Fig. 13. XRD patterns of sludge (a), Class F fly ash (b), CFA (c), CFA/sludge with 0–8% (w/w) Na_2SO_4 (d–g), and CFA with 8% (w/w) Na_2SO_4 (h).

of thin (a few tenths of a micrometer thick) platelets with poorly defined edges. Figure 14 shows that in LFA/sludge with 2% sodium sulfate, prismatic ettrin-

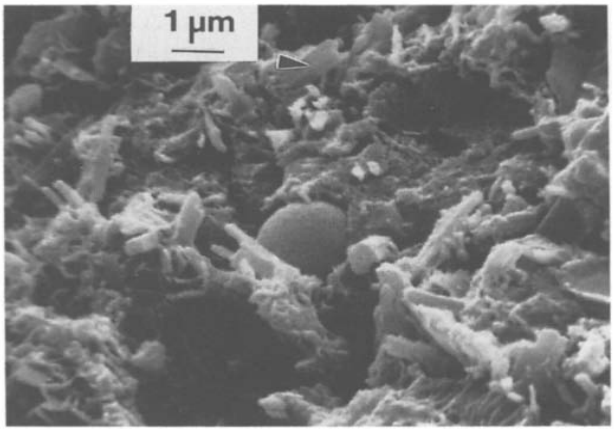

Fig. 14. SEM picture of sludge stabilized with lime/Class C fly ash treated with 2% (w/w) Na_2SO_4. Note the prismatic ettringite crystals.

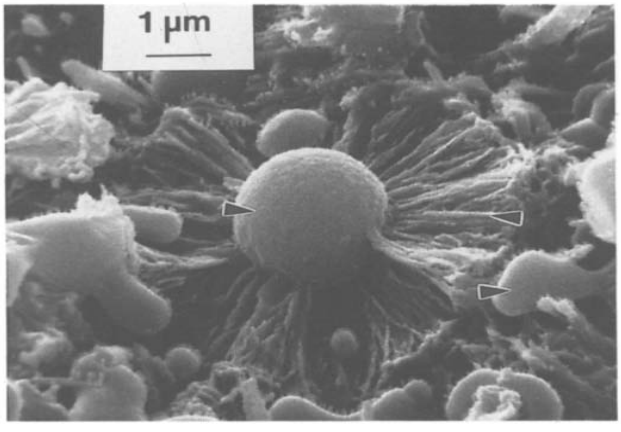

Fig. 15. As Fig. 14, but with 5% (w/w) Na_2SO_4 added. The lower right arrow indicates one of the newly formed microstructures, the thin isolated plates having a smooth contour.

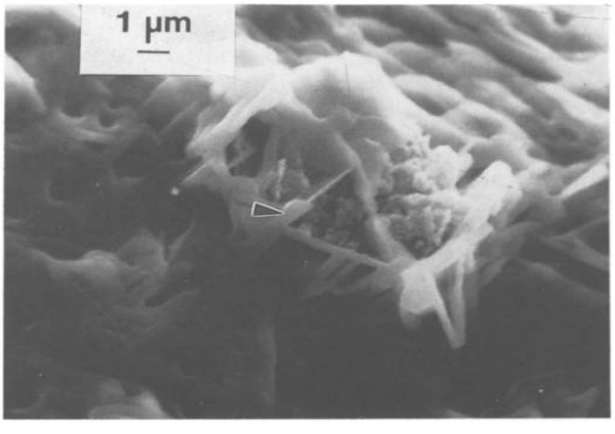

Fig. 16. As Fig. 14, but with 8% (w/w) Na_2SO_4 added. Note the reaction rims around the fly ash particles.

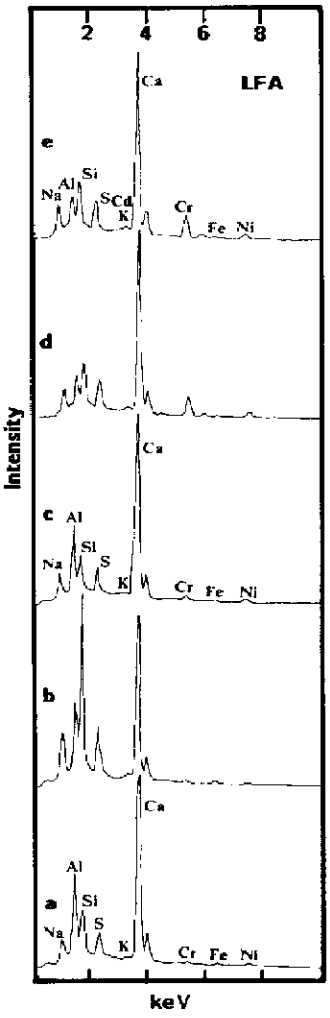

Fig. 17. Energy dispersive X-ray analysis of (a) ettringite from LFA/sludge treated with 5% (w/w) Na_2SO_4, (b) the leaf-like form of Fig. 15, (c) the flat needles of Fig. 16, and (d) the reaction product around a fly ash sphere from treatment with 2% (w/w) Na_2SO_4. In (e) a representative EDX analysis of the (d) sample is depicted.

gite crystals became more common. The change in microstructure was more evident in the 5% sample in which several new forms were observed. One consisted of thin, isolated plates with a gentle wavy outline (Fig. 15, lower right arrow), and another of thin flat needles, as shown in the photomicrograph of LFA/sludge 8% sodium sulfate (Fig. 16). Reaction rims around fly ash spheres became more common with increasing sodium sulfate concentration (Fig. 16).

The addition of sodium sulfate to LFA/sludge resulted in the formation of new phases with its associated crystalline forms. These new crystalline forms depended on the binder composition, and those found in LFA/sludge were dif-

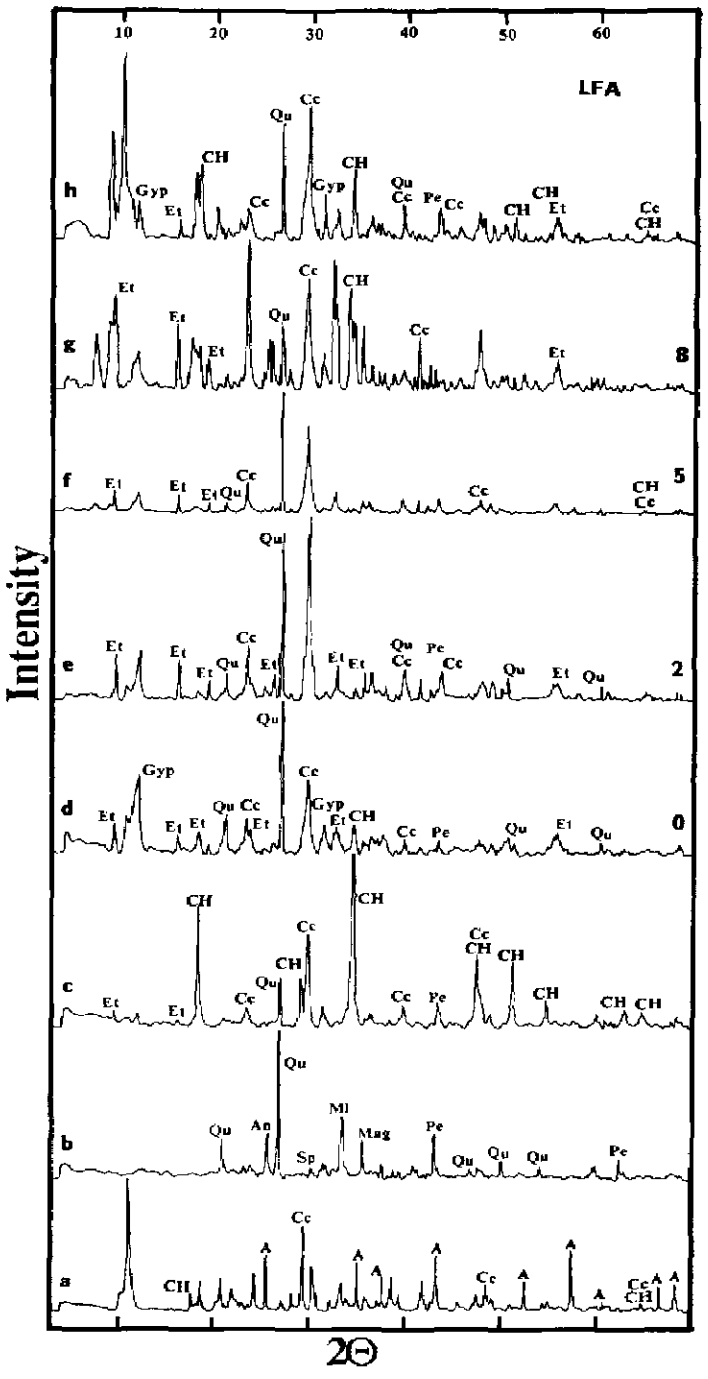

Fig. 18. XRD patterns of sludge (a), Class C fly ash (b), LFA (c), LFA/sludge treated with 0–8% (w/w) Na_2SO_4 (d–g), and LFA treated with 8% (w/w) Na_2SO_4 (h). Three groups of phases can be discerned (see text).

ferent from those in OPC/sludge or CFA/sludge, except for prismatic ettringite which was common in all binders.

An analysis of ettringite from LFA/sludge with 5% sodium sulfate is shown in Fig. 17(a) It was a calcium aluminosulfate with significant amounts of Si and Na; Cr and Ni were also present. Analyses of the leaf-like form (Fig. 15) and flat needles (Fig. 16) are shown in Figs. 17(b) and 17(c), respectively. Both have the same elements as the earlier analysis, but in different proportions. An analysis of the reaction product around a fly ash sphere from LFA/sludge with 2% sodium sulfate, such as shown in Fig. 15, is shown in Fig. 17(d). All of the elements common to the LFA/sludge sodium sulfate system were present. A representative EDX analysis of a fly ash sphere from the above sample is shown in Fig. 17(e). In general, the fly ash spheres were calcium aluminosilicates, but contained minor amounts of Cr and Ni. The amounts of Na and S on fly ash surfaces increased proportionately with sodium sulfate concentration.

Figure 18 shows XRD patterns of (a) sludge, (b) Class C fly ash, (c) LFA, (d–g) LFA/sludge with 0–8% sodium sulfate, and (h) LFA with 8% sodium sulfate. The phases observed in the XRD patterns of LFA/sludge with increasing amounts of sodium sulfate fell into three groups:

1. From the Class C fly ash.
2. Those due to hydration of the binder.
2. Those from the sludge.

Quartz, periclase and occasionally magnetite, were identified from the fly ash, as seen in Fig. 18(b). Calcium hydroxide was present in all samples, and ettringite was also present in all samples, the amount increasing with increasing sodium sulfate concentration. Gypsum and α-$CaSO_4$ ([6], JCPDF 26-0328) were tentatively identified in LFA/sludge 8% sodium sulfate; hydrogarnet (C_3AH_6) was also found. LFA with 8% sodium sulfate contained ettringite, gypsum and monosulfate. Calcium hydroxide was also present. A comparison of the XRD patterns of sludge, LFA, LFA/sludge with 0–8% sodium sulfate, and LFA with 8% sodium sulfate shows that LFA/sludge contained several sludge peaks; however, the intensities varied.

4. Discussion

Many chemical compounds, both inorganic and organic, interfere with the setting process of OPC and other pozzolans [7]. For example, Alexander and Davis [8] reported that when the alkali content in OPC increased from 0.15 to 2.8 wt% the unconfined compressive strength was reduced by 56%. The U.S. EPA requires that a solidified/stabilized waste exhibit at least 3.45 kPa (50 psi) unconfined compressive strength. A commercial process usually attempts to incorporate as much waste as possible without going below the strength limit. Thus a sludge content of 60 to 75% by weight is not uncommon. If an

interfering compound adversely affects the unconfined compressive strength of a binder, it is commonly counteracted by reducing the amount of waste. Of greater concern, however, is the possibility that the interfering compound reacts with the waste itself and makes it more soluble.

The effect of sodium sulfate on cementitious binders is chemically similar to sulfate attack in concrete. However, in our study the source of sulfate is internal and is available during the setting process, whereas the source of the sulfate associated with sulfate attack is external and supplied after the binder has set. During sulfate attack even low levels of sulfate are dangerous: a 2% solution of sodium sulfate is considered strong and can lead to severe deterioration of OPC [9].

In our study, the addition of the interfering compound sodium sulfate did not significantly alter the chemical species present in the sludge. The XRD patterns showed that most of the sludge species could be identified, irrespective of the binder, even in the presence of 8% sodium sulfate. Thus the methods used in this study suggests that physical encapsulation remained the principal method for immobilization of the electroplating waste, although some chemical entrapment may have occurred. Heavy metals did not completely precipitate from the initial solution due to complexing and some remained in the liquid portion of the sludge. Subsequent mixing of the sludge with the binder materials trapped the metals in the matrix and the new phases of the binders.

The degree of hydration was lower in OPC and CFA, as indicated by the greater amounts of C_3S and C_2S observed by XRD. However, it is was not possible to determine whether the sludge or sodium sulfate affected hydration.

Significant changes in microstructure were observed in binders with sludge and sodium sulfate. The effect was most evident on OPC/sludge, where a new cubic crystal form was observed even at the 2% sodium sulfate level. LFA/sludge showed increasing amounts of leaf-like and needle-like crystals with increasing sodium sulfate concentration, and fly ash spheres also showed increased reaction. The amount of ettringite increased in all binders with increasing sodium sulfate concentration. Jawed and Skalny [10] in their review on the effect of alkalies in cement found that, in general, the presence of alkalis led to a greater crystalline fraction. In the presence of sludge the ettringite crystals were thicker and longer. Comparison of the microstructure of the binders at the same sodium sulfate level (8%) shows that the sludge made the binders more crystalline.

Chemical analyses of the new crystal forms indicated that they contained all the elements present in the binders, minor amounts of the heavy metals, and the interfering compound, when present. Even for a single crystal form, the composition was variable from one crystal to another, and different crystal forms had overlapping compositions. For example, in OPC/sludge with 2% sodium sulfate the composition of the cubic crystal form was indistinguishable

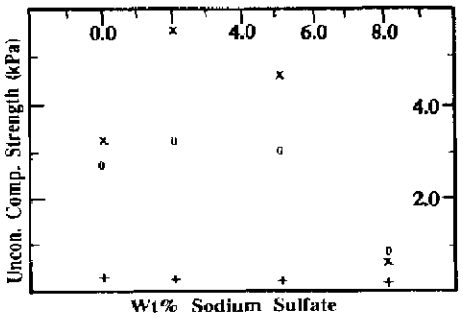

Fig. 19. Effect of sodium sulfate on the unconfined compressive strength of the binders (adapted from Ref. [5]).

from the prismatic hexagonal ettringite crystals. In ettringite, Si can replace Al [11], and some carbonate replacement is also possible.

Our EDX analyses show that in addition to Si, ettringite crystals contained significant amounts Na, Cr and Ni (C could not be detected by this instrument). XRD indicated sodium sulfate was absent in all samples. Thus it reacted with the binders to form new phases. The failure of OPC during sulfate attack is usually attributed to the large increase in volume due to ettringite formation [7]. If instead of ettringite, a different crystalline phase of a very similar chemical composition forms, its expansive properties may be different from that of ettringite and the resultant properties of the binder may also be different. The binder also serves as an immobilizing agent for the interfering compound.

The fly ash spheres in CFA and LFA exchanged significant quantities of material with the surrounding matrix. Class F fly ash in CFA/sludge gained considerable amount of Ca, Na and S, along with minor amounts of Cr and Ni. Class C fly ash in LFA/sludge indicated similar exchanges. Analyses of the fly ash spheres were often indistinguishable from the surrounding matrix.

Calcium hydroxide was observed by XRD in OPC/sludge and LFA/sludge, but was absent in CFA/sludge irrespective of sodium sulfate concentration. The presence of calcium hydroxide in OPC/sludge and LFA/sludge should restrict their pH to approximately 12.6, but it could be lower in CFA/sludge. The solubility of most metal hydroxides is usually lowest around pH 10 [12]. Thus the CFA system may be better suited for S/S than others. However, an acidic environment can be counteracted for a longer period of time by the calcium hydroxide in OPC and LFA.

The effect of sodium sulfate on the unconfined compressive strength of the binders is shown in Fig. 19 (adapted from [5]). The addition of 2% sodium sulfate produced an increase in the strength of LFA/sludge, but had little impact on CFA/sludge or OPC/sludge. In general, the strength of the binders decreased with increasing sodium sulfate concentration. It should be noted

that the very presence of the sludge drastically reduced the unconfined compressive strength of OPC. A 2 wt% concentration of sodium sulfate in CFA/sludge and LFA/sludge did not exhibit a noticeable difference in microstructure, but the difference was quite apparent in OPC/sludge.

A correlation between strength and the amount of amorphous and crystalline phases, and porosity has been observed in cementitious binders (e.g. [13,14]). In the present study, though it is difficult to quantify each, unconfined compressive strength decreased with increasing crystalline fraction. This study shows that CFA and LFA are better S/S agents than OPC for the combination of sludge and interfering compound investigated.

In the present study, the chemical species in the sludge remained practically unaltered with increasing sodium sulfate concentration (and the attendant change in strength). If the sludge species, and thus their solubilities, remained unchanged, no correlation is expected between leaching characteristics and strength, or sodium sulfate concentration. The observation agrees with the data in the literature on the absence of any correlation between leaching and unconfined compressive strength [15].

5. Conclusions

Physical encapsulation was the principal mechanism for immobilizing the heavy metal sludge. Sodium sulfate did not significantly affect the nature of the sludge species.

Sodium sulfate reacted with the binders to produce phases with crystalline forms different from the same system without sodium sulfate. No crystalline form was common between any two sludge-containing binders, except prisms of ettringite. However, compositions of the crystalline forms were indistinguishable from each other. The amount of ettringite increased with increasing sodium sulfate concentration irrespective of binder. At the same sodium sulfate level, all binders had a higher fraction of crystalline phases in the presence of sludge.

A strong correlation existed between unconfined compressive strength and the fraction of crystalline compounds. The continuous decrease in unconfined compressive strength of OPC was due to the increasing crystalline fraction with increasing sodium sulfate content. The final low strengths were due to the higher fractions of crystalline compounds.

References

1 J.R. Conner, Chemical Fixation and Solidification of Hazardous Wastes, Van Nostrand Reinhold, New York, HY, 1990, pp. 692.
2 M.B. Walsh, Hazard. Waste Hazard. Mater., 3 (1986) 1.

3 D.G. Skipper, H.C. Eaton, F.K. Cartledge and M.E. Tittlebaum, Cem. Concr. Res., 17 (1987) 851.
4 A. Roy, H.C. Eaton, F.K. Cartledge and M.E. Tittlebaum, Hazard. Waste Hazard. Mater., 8 (1991) 33.
5 J.M. Cullinane, R.M. Bricka and N.R. Francingues, 13th Annu. EPA Res. Symp., Cincinnati, OH, 1987, pp. 64.
6 JCPDS, Powder Diffraction File, International Center for Diffraction Data, Swarthmore, PA, 1986.
7 F.M. Lea, The Chemistry of Cement and Concrete, Chemical Publ. Co., New York, NY, 1987, pp. 727.
8 K.M. Alexander and C.E.S. Davis, Aust. J. Appl. Sci., 11 (1960) 1.
9 G.L. Kalousek, Cem. Concr. Res., 2 (1972) 79.
10 I. Jawed and J. Skalny, Cem. Concr. Res., 8 (1978) 37.
11 W. Lukas, Cem. Concr. Res., 6 (1976) 225.
12 J.W. Patterson, Industrial Wastewater Treatment Technology, Butterworth, Boston, MA, 1985, 467 pp.
13 R.F. Feldman and J.J. Beaudoin, Cem. Concr. Res., 6 (1976) 389.
14 J.J. Beaudoin and R.F. Feldman, Cem. Concr. Res., 15 (1985) 105.
15 U.S. Environmental Protection Agency, Stabilization/Solidification of CERCLA and RCRA Wastes, Physical Tests, Chemical Testing Procedures, Technology Screening, and Field Activities. EPA/625/6-89/022, EPA, Cincinnati, OH, 1989.